Activated rate processes in a double well coupled to a slow harmonic mode: Finite-barrier effects

Alexander N. Drozdov* and Peter Talkner
Paul Scherrer Institute, CH-5232 Villigen, Switzerland
(Received 15 May 1996)

Activated rate processes of a reactive coordinate in a symmetric double well coupled to a harmonic mode are studied in the limit of large damping. The transition rate is given by the least nonvanishing eigenvalue of the corresponding two-dimensional Smoluchowski equation. This eigenvalue is numerically determined for four different temperatures and various different coupling and anisotropy parameters and compared with the value of the Rayleigh quotient for the trial function following from the Kramers-Langer theory. Deviations between the numerically exact rates and Kramers-Langer theory are due to finite-barrier heights and may become very large in the case of a slow harmonic mode, i.e., large anisotropy. As long as these deviations are not too large, the rate expression obtained from the Rayleigh quotient is in excellent agreement with the numerically exact results. The stochastic separatrix is numerically determined as the node of the eigenfunction corresponding to the least nonvanishing eigenvalue and compared to results from a perturbation theory.
[S1063-651X(96)09112-X]

PACS number(s): 05.40.+j, 82.20.Db

I. INTRODUCTION

The thermally activated escape over a barrier represents a decisive step in the dynamics of various processes in physics, chemistry, and biology [1,2]. The role of the interaction of the considered system with a surrounding heat bath was recognized and fully taken into account for a simple model by Kramers [1]. He considered a single mechanical particle in a bistable potential that interacts with a heat bath. The heat bath causes a velocity proportional friction force and a random force, the former extracting and the latter supplying energy. The correlation time of the random force is supposed to be vanishingly small such that a Markovian process results for the considered system. This assumption is not always met in physical applications. Therefore, generalizations to higher-dimensional [3–6] and non-Markovian [7,8] systems have been put forth. All these theories, which will be subsumed under the name Kramers-Langer theory, are generalizations of Kramers's spatial diffusion regime where the coupling of the system to the bath is strong enough such that energy is efficiently exchanged between system and bath. Energy diffusion limited rates for generalized Langevin equations are treated in Ref. [9] and for multidimensional problems in [10], but will not be considered here. The Kramers-Langer theory is correct, when the barrier height $V^{\ddagger}$ is large compared to the thermal energy β^{-1}. The actual value of $\beta V^{\ddagger}$ for which it applies depends on the considered system. In particular, the presence of other small or large parameters may render the Kramers-Langer theory inapplicable for all physically relevant barrier heights as has been found for a model with exponential memory friction for both a large bath correlation time and large static friction [8,11].

A generalization of this model has been put forth for charge-transfer reactions in polar solvents [12]. There the relaxation time of the solvent polarization may be very different from the one of the reactive coordinate. Within a simple model, the polarization is described by a single solvation coordinate y, which couples to the reactive coordinate x through the potential of mean force $V(x,y)$, reading

$$V(x,y)=U(x)+\frac{\Gamma}{2}[y-y_{\mathrm{eq}}(x)]^2, \tag{1}$$

where $U(x)$ is a double-well potential, $y_{\mathrm{eq}}(x)$ is the equilibrium polarization at the given value x of the reactive coordinate, and Γ is the coupling constant. When the motion of the remaining degrees of freedom that make up the heat bath at temperature β^{-1} are fast, the dynamics can be modeled in terms of the coupled Langevin equations

$$\ddot{x}=-\partial_x V(x,y)-\eta_x\dot{x}+\sqrt{2\eta_x/\beta}f_x(t),$$
$$\ddot{y}=-\partial_y V(x,y)-\eta_y\dot{y}+\sqrt{2\eta_y/\beta}f_y(t), \tag{2}$$

where η_x and η_y are the damping constants in the directions of the reaction and solvation coordinates, respectively, and $f_x(t)$ and $f_y(t)$ are independent Gaussian white random forces with zero mean values

$$\langle f_x(t)\rangle=\langle f_y(t)\rangle=\langle f_x(t)f_y(s)\rangle=0,$$
$$\langle f_x(t)f_x(s)\rangle=\langle f_y(t)f_y(s)\rangle=\delta(t-s). \tag{3}$$

In the limit of large damping constants η_x and η_y, the velocities $\dot{x}$ and $\dot{y}$ relax fast and a two-dimensional Markovian process results that is governed by a Smoluchowski equation. It reads

$$\partial_t P(x,y,t)=LP(x,y,t), \tag{4}$$

where

$$L=D(\partial_x e^{-V/D}\partial_x e^{V/D}+\varepsilon\partial_y e^{-V/D}\partial_y e^{V/D})P(x,y,t) \tag{5}$$

*Present address: Universidad de Sevilla, Física Teórica, Apartado Correos 1065, Sevilla 41080, Spain. Permanent address: Institute for High Temperatures, 13/19 Izhorskaya Street, 127412 Moscow, Russia.

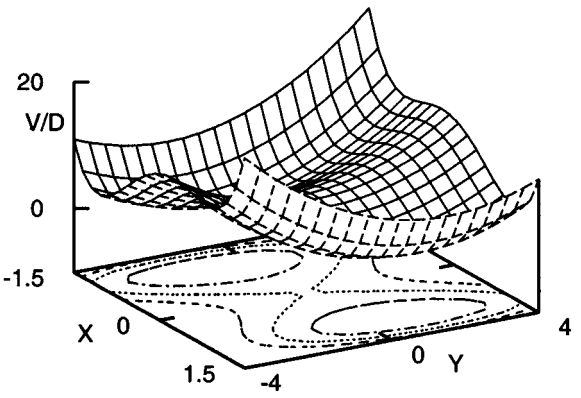

FIG. 1. Potential surface $V(x,y)/D$ [Eq. (5)] and its equipotential lines for $D=0.05$ and $\gamma=0.05$.

denotes the Smoluchowski operator. Here dimensionless variables have been introduced. In particular, time is measured in units of η_x^{-1}, $\varepsilon=\eta_x/\eta_y$ denotes the anisotropy parameter, and D is a dimensionless temperature.

In another paper [13], we have studied this model for the potential

$$V(x,y)=U(x)+\frac{\gamma}{2}(y-x)^2,$$

$$U(x)=\frac{1}{4}x^4-\frac{1}{2}x^2, \tag{6}$$

which has two minima at $(-1,-1)$ and $(1,1)$ and a saddle point at the origin. The barrier height measured in units of the thermal energy of the bath is $\beta V^{\ddagger}=E=(4D)^{-1}$. A typical shape of the potential surface and its equipotential lines are shown in Fig. 1.

For most of the parameter values the transition rate from one minimum to the other is half of the least nonvanishing eigenvalue λ_1 of the Smoluchowski operator L defined in (5). Using a suitable set of basis functions, this eigenvalue has been calculated in [13] for different values of the reduced barrier height E, dimensionless coupling constant γ, and anisotropy parameter ε. A comparison of the numerically exact least eigenvalue and the result from the Kramers-Langer theory shows good agreement when the coupling parameter γ is large. If γ is of the order of $U''(x=1)$ or smaller and $E=10$ or smaller the agreement becomes worse. In particular, when the anisotropy parameter ε additionally becomes small the Kramers-Langer theory completely breaks down.

The mathematical reason for this breakdown is the presence of up to three small parameters D,ε, and γ. Though the limit of the least eigenvalue is always zero, independently of the order in which the parameters D,ε, and γ vanish, the asymptotic behavior crucially depends on the relative order of these parameters. If, for example, the diffusion constant D is the smallest parameter, the smallest nonvanishing eigenvalue is well separated from the others and given by the Kramers-Langer expression for the transition rate between the two metastable states of the potential. It consequently is of Arrhenius type with an activation energy given by the barrier height at the saddle point. If, however, the anisotropy ε is the smallest parameter and the coupling γ is finite but not too large, a slow one-dimensional motion in the y direction in an effective double-well potential results, which has a smaller barrier height than the bare potential [13]. The long-time behavior is then also governed by a single Arrhenius-type eigenvalue but with a smaller activation energy than that following from the bare potential. Another extreme case occurs if the coupling constant γ approaches zero first. Then the y coordinate is also slow and a densely spaced spectrum of almost equidistant eigenvalues determines the long-time behavior. In particular, the breakdown of the Kramers-Langer theory in the anisotropic friction limit was discussed in a number of papers [14–17].

In this paper, we compare numerically exact least eigenvalues with results from the Rayleigh quotient for Kramers-Langer-type trial functions. In this way finite barrier corrections are systematically studied. This leads to much better results for all cases where the relative deviation between the Kramers-Langer rate and the numerically exact rate is less than approximately 50%. In cases where the Kramers-Langer theory fails completely the finite-barrier corrections also do not yield valid results. By means of a perturbation theory the Kramers-Langer trial function systematically can be improved [18,19]. While the node line of the original Kramers-Langer trial function coincides with the deterministic separatrix at the saddle, the node line of the improved trial function better approximates the true stochastic separatrix [20].

Before closing this Introduction we note that the problem of finite-barrier corrections for the rate actively has been studied in recent years and many different methods have been suggested for their evaluation [6,19,21–23]. In this paper, we will use a perturbation expansion in combination with the Rayleigh quotient [19]. The central advantages of this approach are that, first, it yields approximate eigenvalues that possess the property of being an upper bound, second, it allows one to systematically construct perturbation corrections to the conventional Kramers-Langer trial function, and, third, a first-order error in the trial function leads to a second-order error in the estimate for the rate. The paper is organized as follows. In Sec. II the Rayleigh quotient and the perturbation theory are presented. The numerical method is reviewed in Sec. III and the results are compared in Sec. IV. Section V ends the paper with an outlook.

II. PERTURBATION THEORY

In this section the Kramers-Langer theory is briefly reviewed within the scope of the Rayleigh quotient method and then a perturbation theory for the Kramers function is developed.

A. Langer's formula

As we have already noted, we treat the equilibration process of the considered system by means of the eigenvalue-problem of the Smoluchowski operator defined by (5), that is,

$$LP_n(x,y)=-\lambda_n P_n(x,y). \tag{7}$$

It is well known [24] that a process governed by a Smoluchowski equation obeys strict detailed balance, i.e.,

$$L(P_0 f) = P_0 L^+ f \tag{8}$$

for any smooth function f, where

$$P_0(x,y) = \exp\{-V(x,y)/D\} \Big/ \int_{-\infty}^{\infty} dx\, dy \times \exp\{-V(x,y)/D\} \tag{9}$$

denotes the equilibrium distribution satisfying $LP_0 = 0$ and L^+ denotes the backward operator

$$L^+ = De^{V/D}(\partial_x e^{-V/D}\partial_x + \varepsilon\,\partial_y e^{-V/D}\partial_y). \tag{10}$$

As a consequence of (8), L^+ is a Hermitian operator with respect to the scalar product of functions $f(x,y)$ and $g(x,y)$ defined by

$$(g,f) = \int_{-\infty}^{\infty} dx\; dy P_0(x,y) g(x,y) f(x,y). \tag{11}$$

Therefore, a complete orthogonal set of eigenfunctions $\{Q_n\}$ exists with corresponding real eigenvalues λ_n that are non-negative [24]

$$(Q_n, Q_m) = \delta_{n,m},$$
$$L^+ Q_n = -\lambda_n Q_n. \tag{12}$$

Equation (8) further entails that L has the same eigenvalues λ_n with the corresponding eigenfunctions $P_n = Q_n P_0$. Obviously, $Q_0 = 1$ is an eigenfunction with corresponding eigenvalue $\lambda_0 = 0$.

Here we are interested mainly in the least nonvanishing eigenvalue λ_1 (for notational simplicity we will drop from here on the index 1 whenever no confusion may arise). For this eigenvalue, the Rayleigh quotient

$$\lambda = -\frac{(Q, L^+ Q)}{(Q,Q)} \tag{13}$$

provides an upper bound if Q is orthogonal on $Q_0 = 1$, i.e., $(Q,1) = 0$. In order to construct a trial function we use the fact that the least eigenvalue is small and hence may be neglected in the eigenvalue problem, i.e.,

$$L^+ Q = 0. \tag{14}$$

For vanishing diffusion the resulting first-order partial differential equation has only solutions that are piecewise constant on the domains of attraction of the deterministic equations of motion. We choose these values as being $+1$ and -1, such that the resulting function is orthogonal on the overall constant function. The presence of small diffusive terms in L^+ changes the behavior of Q only near the deterministic separatrix where the steplike behavior is smoothed out. Since the Rayleigh quotient contains the stationary distribution as a weight, only the region of the saddle point is of importance for sufficiently small D. Hence we may split the backward operator into a leading contribution L_0^+ and a correction L_1^+ reading

$$L^+ = L_0^+ + L_1^+, \tag{15}$$

where

$$L_0^+ = [(1-\gamma)x + \gamma y]\partial_x + D\partial_{xx}^2 + \varepsilon\,\gamma(x-y)\partial_y + \varepsilon D\partial_{yy}^2 \tag{16}$$

describes the linear dynamics near the saddle and

$$L_1^+ = -x^3 \partial_x \tag{17}$$

the anharmonic correction. In passing we note that rescaling the coordinates x and y by the inverse square root of the barrier height renders the leading contribution L_0^+ independent of the diffusion constant D and the correction L_1^+ proportional to the inverse barrier height. Hence the inverse barrier height may be considered as the formal smallness parameter in the following perturbation theory. The solution of the unperturbed problem

$$L_0^+ Q_{(0)} = 0 \tag{18}$$

is known from the Kramers-Langer theory. It reads

$$Q_{(0)}(x,y) = \sqrt{\frac{2}{\pi}} \int_0^{\sqrt{b}(wx+y)} du \exp\{-u^2/2\}, \tag{19}$$

where

$$b = \frac{\kappa}{D(\varepsilon + w^2)}, \tag{20}$$

$$w = \varepsilon + \frac{\kappa}{\gamma}, \tag{21}$$

and

$$\kappa = \frac{1}{2}\{1 - \gamma - \gamma\varepsilon + [(1-\gamma-\gamma\varepsilon)^2 + 4\gamma\varepsilon]^{1/2}\}. \tag{22}$$

The result of Eq. (19) used as a trial function in the Rayleigh quotient yields, in leading order in D,

$$\lambda_{\mathrm{KL}} = \frac{\sqrt{2}}{\pi}\kappa \exp\{-E\}. \tag{23}$$

This coincides with twice the Kramers-Langer rate [4] and is therefore distinguished from the other expressions for the eigenvalue by the subscript KL.

Now, let us briefly analyze the dependence of λ_{KL} on the coupling constant and anisotropy parameter. These parameters enter (23) only through the transmission factor (22). This factor tends to unity for all positive γ's if the anisotropy parameter goes to infinity. Note that in the original units of (2) for fixed η_y the rate tends to zero as $1/\eta_x$ with increasing η_x. On the other hand, in the limit of vanishingly small anisotropy parameters (in the following this limiting case will be referred to as *strongly anisotropic* limit) there are three regimes with a different dependence of λ_{KL} on ε. When γ is larger than unity, λ_{KL} is linear in ε, i.e., $\kappa \simeq \varepsilon\gamma/(\gamma-1)$. At $\gamma = 1$ it also tends to zero as the square root of ε, $\lambda_{\mathrm{KL}} \sim \sqrt{\varepsilon}$. Finally, if the coupling constant is less than unity, the transmission factor tends to the finite value $\kappa = 1 - \gamma$. This, however, does not coincide with the behav-

ior of the least nonvanishing eigenvalue, which must always linearly vanish with ε [13]. Thus one may expect considerable deviations of the Kramers-Langer theory from numerically exact results in the limit $\varepsilon \to 0$ for all positive $\gamma \leqslant 1$. Therefore, much of the work dealing with activated rate processes in systems coupled to slow harmonic modes [14,16] is concerned with estimates for the rate in the limit of vanishingly small ε.

Our results of Ref. [13] show first, that $\gamma = 1$ is not a strict limit of validity of the Kramers-Langer theory—rather, the latter fails for sufficiently small ε also if γ is larger than unity, and, second, that the Kramers-Langer theory also fails near the isotropic case $\varepsilon \sim 1$ if the barrier height is not too large and γ is of order unity. We also found that the theory may break down even for $\varepsilon > 1$ due to the smallness of the coupling constant. In this limit the transmission factor κ in (23) approaches unity corresponding to the motion in the bare reactive potential $U(x)$ and does not reflect the slow relaxation of the y coordinate on the time scale γ^{-1}. This case is not particularly interesting since then the reactive system is practically decoupled from the extremely slow y mode.

In those cases when the reactive mode determines the long-time dynamics the observed deviations of the rate from the Kramers-Langer theory are due to the fact that the trial function (19) only is exact for a parabolic barrier and that also anharmonic contributions that are contained in the weight of the scalar product (13) are neglected; see also (11).

B. Finite-barrier corrections

Based on the decomposition of the backward operator (15), a perturbation theory for the trial function can be performed leading to the series representation [18,19]

$$Q(x,y) = Q_{(0)}(x,y) + Q_{(1)}(x,y) + Q_{(2)}(x,y) + \cdots, \quad (24)$$

where $Q_{(0)}(x,y)$ is determined by (19), while all higher contributions recursively follow from a hierarchy of inhomogeneous equations of the form

$$L_0^+ Q_{(k)}(x,y) = -L_1^+ Q_{(k-1)}(x,y), \quad k \geqslant 1. \quad (25)$$

Inserting (24) into (13), we find the estimate of the rate

$$\lambda^{(k+1)} = \lambda^{(k)} \frac{N_{k+1}}{N_k} - \frac{(Q_{(k)}, L_1^+ Q_{(k-1)})}{N_{k+1}} - \frac{(Q_{(k)}, L_1^+ Q_{(k)})}{N_{k+1}},$$

$$N_k = (Q_{(0)} + \cdots + Q_{(k)}, Q_{(0)} + \cdots + Q_{(k)}), \quad (26)$$

where $\lambda^{(0)} = 0$, $Q_{(-1)} = 0$, and $N_0 = (Q_{(0)}, Q_{(0)})$. The result $\lambda^{(k)}$ is correct up to order $2k-1$ in the perturbation, i.e., up to the order E^{-2k+1}. Usually, one argues that all N_k are unity up to exponentially small corrections in the barrier height, and therefore can be neglected. We will see in the following that for low barrier heights these corrections also become important. Note that all $\lambda^{(k)}$ represent upper bounds of the true eigenvalue λ_1.

In the present paper, we will not go beyond first order in the perturbation L_1^+. It is not difficult to obtain the rate including the first correction

$$\lambda^{(1)} = \frac{2\kappa}{\pi N_0 \sqrt{\alpha}} \frac{\int_{-\infty}^{\infty} dx \exp\{-(x^4 + 2x^2/\alpha + 1)/4D\}}{\int_{-\infty}^{\infty} dx \exp\{-(x^2-1)^2/4D\}}, \quad (27)$$

where

$$\alpha = 1 + 2Db/\gamma. \quad (28)$$

If $D < 0.05$ the scalar product N_0 can be approximated by unity. The error of this approximation is of the order $D \exp -4/D$. If, further, $\alpha^2 D \leqslant 0.1$ one can simplify the above formula by deexponentiating $\exp\{-x^4/4D\}$ and keeping only terms that contribute up to first order in D (in the inverse barrier height)

$$\exp\left\{-\frac{x^4}{4D}\right\} = 1 - \frac{x^4}{4D} + \cdots.$$

In the indicated parameter regime the error of this approximation is at most 2%. The integrations can be performed analytically, yielding the expression

$$\lambda_{\mathrm{RQ}} = \lambda_{\mathrm{KL}}\left[1 - \frac{3}{4} D(1+\alpha^2)\right]. \quad (29)$$

where the index RQ indicates the result of the Rayleigh quotient up to first order in D. Note that according to its definition (20) b, and consequently α, diverges at $\gamma = 1$ and $\varepsilon = 0$. Further, it must be pointed out that the bounding property of the Rayleigh quotient may be lost both when N_0 is approximated by unity and when the numerator and the denominator of (27) are asymptotically evaluated.

Next, we determine the first-order corrections of the Kramers-Langer trial function (19) with the aim of finding the precise location of the stochastic separatrix in the vicinity of the saddle point. For this purpose it is convenient to split off a Gaussian function from $Q_{(1)}$,

$$Q_{(1)}(x,y) = \sqrt{\frac{2b}{\pi}} F(x,y) \exp\left\{-\frac{1}{2} b(wx+y)^2\right\}. \quad (30)$$

Then Eq. (25) yields

$$[L_0^+ - 2bD(wx+y)(\partial_x + \varepsilon \partial_y) - \kappa] F = wx^3. \quad (31)$$

The above equation can exactly be solved by expanding F in powers of x and y,

$$F(x,y) = Ax + By + Cx^3 + Gx^2 y + Rxy^2 + Sy^3. \quad (32)$$

Inserting (32) into (31) and equating like powers in x and y gives

$$R=\frac{\kappa+3\varepsilon\gamma\alpha}{\gamma-2bw}S,$$

$$G=\frac{\kappa-1+\gamma+2\varepsilon\gamma\alpha+2bw^2}{2(\gamma-2bw)}R-\frac{3}{2}\varepsilon S,$$

$$C=\frac{\kappa-2+2\gamma+\varepsilon\gamma\alpha+4bw^2}{3(\gamma-2bw)}G-\frac{2}{3}\varepsilon R,$$

$$B=\frac{(1-\gamma-\kappa-2bw^2)(2G+6\varepsilon S)-(\gamma-2bw)(2\varepsilon R+6C)}{\varepsilon(\gamma-2bw)^2+(1-\gamma-\kappa-2bw^2)(\kappa+\varepsilon\gamma\alpha)},$$

$$A=\frac{(\kappa+\varepsilon\gamma\alpha)B-2G-6\varepsilon S}{\gamma-2bw},$$

$$\begin{aligned}S=w(\gamma-2bw)\Bigg\{&\frac{2}{3}\varepsilon(\kappa+3\varepsilon\gamma\alpha)(\kappa+3\gamma-3+6bw^2)\\&+[(\kappa+3\varepsilon\gamma\alpha)(\kappa+2\gamma-1+2\varepsilon\gamma\alpha+2bw^2)\\&-3\varepsilon(\gamma-2bw)^2]\Bigg[\frac{\varepsilon}{2}\\&-\frac{(\kappa+3\gamma-3+6bw^2)(\kappa+2\gamma-2+\varepsilon\gamma\alpha+4bw^2)}{6(\gamma-2bw)^2}\Bigg]\Bigg\}^{-1}.\end{aligned}\tag{33}$$

Hence, in first-order perturbation theory the trial function reads

$$\begin{aligned}Q(x,y)=\sqrt{\frac{2b}{\pi}}\Bigg[&\int_0^{wx+y}du\,\exp\left\{-\frac{b}{2}u^2\right\}\\&+F(x,y)\exp\left\{-\frac{b}{2}(wx+y)^2\right\}\Bigg].\end{aligned}\tag{34}$$

By definition, the probabilities of going in either direction of reactants and products are equal for trajectories that start from the stochastic separatrix. One can show [19,20] that the stochastic separatrix coincides with the node line of the eigenfunction belonging to the least nonvanishing eigenvalue provided it is the relevant eigenvalue characterizing the considered transition. Using for the eigenfunction the result (34), we obtain as an equation for the stochastic separatrix

$$Q(x,y_{\rm SS})=0.\tag{35}$$

This equation can be solved for $y_{\rm SS}$ numerically. In the vicinity of the origin an approximate analysis yields

$$y_{\rm SS}(x)=-(A+w-Bw)x+(C-Gw+Rw^2-Sw^3)x^3.\tag{36}$$

By contrast, the deterministic separatrix is given in the vicinity of the saddle point by the straight line

$$y_{\rm DS}(x)=-wx,\tag{37}$$

which also has a slope different from that of the stochastic separatrix at $x=0$.

III. BASIS SET METHOD

In this section a basis set method for numerically solving time-independent Smoluchowski and Schrödinger equations is developed. The method is very efficient in dealing with a so-called system-bath situation in which a nonlinear degree of freedom couples to a harmonic bath. For the sake of generality, we consider a harmonic bath with an arbitrary number of modes N governed by the Smoluchowski operator

$$L=D\left(\partial_x e^{-V/D}\partial_x e^{V/D}+\sum_{i=1}^{N}\varepsilon_i\partial_i e^{-V/D}\partial_i e^{V/D}\right),$$

$$V(x,\mathbf{y})=U(x)+\frac{1}{2}\sum_{i=1}^{N}\gamma_i(y_i-x)^2,\tag{38}$$

where $\mathbf{y}^T=(y_1,\ldots,y_N)$, $\partial_i=\partial_{y_i}$, and $\varepsilon_i=\eta_x/\eta_{y_i}$. First we transform (38) by means of the ansatz

$$P(x,\mathbf{y})=\psi(x,\mathbf{y})\exp\left\{-\frac{V(x,\mathbf{y})}{2D}\right\}\tag{39}$$

into a Hamiltonian operator of the form

$$\begin{aligned}H&=H_x+H_b+H_{xb},\\H_x&=-D\partial_{xx}^2+\frac{U'^2}{4D}-\frac{U''}{2},\\H_b&=\sum_{i=1}^{N}\varepsilon_i\left[-D\partial_{ii}^2+\frac{\gamma_i^2}{4D}(y_i-x)^2-\frac{\gamma_i}{2}\right],\\H_{xb}&=\sum_{i=1}^{N}\frac{1}{2D}[U'(x)\gamma_i(x-y_i)-D\gamma_i]\\&\quad+\frac{1}{4D}\left[\sum_{i=1}^{N}\gamma_i(x-y_i)\right]^2.\end{aligned}\tag{40}$$

This transformation allows us to take advantage of the fact that the matrix representation of a Hamiltonian operator is symmetric. The underlying idea is to determine the generic basis function element as

$$\psi_{\mathbf{n}m}=\chi_m(x)\prod_{i=1}^{N}\varphi_{n_i}(y_i-x),\tag{41}$$

where the products $\Pi_i\varphi_{n_i}(y_i-x)$ are eigenfunctions of the bath Hamiltonian H_b which are given by a set of displaced harmonic oscillators

$$\left\{-D\partial_{ii}^2+\frac{\gamma_i^2}{4D}(y_i-x)^2-\frac{\gamma_i}{2}\right\}\varphi_{n_i}=\gamma_i n_i\varphi_{n_i},\tag{42}$$

while $\chi_m(x)$ are the eigenfunctions of the Hamiltonian operator corresponding to the *uncoupled* reactive subsystem

$$\left(-D\partial_{xx}^2+\frac{U'^2}{4D}-\frac{U''}{2}\right)\chi_m=\mu_m\chi_m.\tag{43}$$

TABLE I. Comparison between Langer's formula λ_{KL} [Eq. (23)], the Rayleigh quotient evaluated in the steepest-descent approximation λ_{RQ} [Eq. (29)] [a bar − indicates a negative value], the full Rayleigh quotient $\lambda^{(1)}$ [Eq. (27)], and the numerically exact results λ for the least nonvanishing eigenvalue of the Smoluchowski operator (5). Exponential notation $[-k]$ means that the preceding number is to be multiplied by 10^{-k}.

		$E=2.5$				$E=5$			
γ	ε	λ_{KL}	λ_{RQ}	$\lambda^{(1)}$	λ	λ_{KL}	λ_{RQ}	$N_0\lambda^{(1)}$	λ
0.5	0.1[−2]	0.185[−1]	0.157[−1]	0.140[−1]	0.6929[−4]	0.152[−2]	0.140[−2]	0.122[−2]	0.1497[−4]
0.5	0.1[−1]	0.187[−1]	0.473[−2]	0.142[−1]	0.6768[−3]	0.153[−2]	0.960[−3]	0.123[−2]	0.1364[−3]
0.5	0.1	0.200[−1]	0.569[−2]	0.160[−1]	0.5529[−2]	0.164[−2]	0.106[−2]	0.137[−2]	0.7853[−3]
0.5	1	0.261[−1]	0.125[−1]	0.234[−1]	0.2046[−1]	0.214[−2]	0.158[−2]	0.192[−2]	0.1839[−2]
0.5	10	0.341[−1]	0.264[−1]	0.321[−1]	0.3078[−1]	0.280[−2]	0.248[−2]	0.256[−2]	0.2553[−2]
0.5	100	0.366[−1]	0.310[−1]	0.347[−1]	0.3321[−1]	0.300[−2]	0.277[−2]	0.276[−2]	0.2749[−2]
1	0.1[−2]	0.115[−2]	0.978[−3]	0.335[−3]	0.5686[−4]	0.944[−4]	0.873[−4]	0.329[−4]	0.7107[−5]
1	0.1[−1]	0.351[−2]		0.171[−2]	0.5567[−3]	0.289[−3]		0.162[−3]	0.6811[−4]
1	0.1	0.998[−2]		0.728[−2]	0.4648[−2]	0.819[−3]		0.647[−3]	0.4977[−3]
1	1	0.228[−1]	0.270[−2]	0.202[−1]	0.1904[−1]	0.187[−2]	0.105[−2]	0.168[−2]	0.1645[−2]
1	10	0.339[−1]	0.267[−1]	0.312[−1]	0.3065[−1]	0.278[−2]	0.249[−2]	0.255[−2]	0.2539[−2]
1	100	0.366[−1]	0.310[−1]	0.339[−1]	0.3321[−1]	0.300[−2]	0.277[−2]	0.276[−2]	0.2748[−2]
1.5	0.1[−2]	0.110[−3]	0.934[−4]	0.704[−4]	0.4963[−4]	0.902[−5]	0.834[−5]	0.643[−5]	0.5133[−5]
1.5	0.1[−1]	0.102[−2]		0.679[−3]	0.4876[−3]	0.838[−4]	0.429[−5]	0.617[−4]	0.4998[−4]
1.5	0.1	0.667[−2]		0.516[−2]	0.4173[−2]	0.548[−3]	0.128[−3]	0.452[−3]	0.4018[−3]
1.5	1	0.215[−1]	0.880[−2]	0.191[−1]	0.1839[−1]	0.176[−2]	0.124[−2]	0.159[−2]	0.1566[−2]
1.5	10	0.338[−1]	0.272[−1]	0.310[−1]	0.3060[−1]	0.277[−2]	0.250[−2]	0.254[−2]	0.2534[−2]
1.5	100	0.366[−1]	0.310[−1]	0.337[−1]	0.3321[−1]	0.300[−2]	0.278[−2]	0.276[−2]	0.2748[−2]
2	0.1[−2]	0.736[−4]	0.626[−4]	0.551[−4]	0.4559[−4]	0.604[−5]	0.559[−5]	0.486[−5]	0.4357[−5]
2	0.1[−1]	0.711[−3]	0.183[−3]	0.538[−3]	0.4489[−3]	0.584[−4]	0.367[−4]	0.474[−4]	0.4269[−4]
2	0.1	0.548[−2]	0.172[−2]	0.445[−2]	0.3905[−2]	0.450[−3]	0.296[−3]	0.384[−3]	0.3581[−3]
2	1	0.208[−1]	0.121[−1]	0.186[−1]	0.1803[−1]	0.170[−2]	0.135[−2]	0.154[−2]	0.1524[−2]
2	10	0.337[−1]	0.275[−1]	0.309[−1]	0.3057[−1]	0.277[−2]	0.251[−2]	0.254[−2]	0.2532[−2]
2	100	0.366[−1]	0.311[−1]	0.336[−1]	0.3321[−1]	0.300[−2]	0.278[−2]	0.276[−2]	0.2748[−2]
3	0.1[−2]	0.553[−4]	0.470[−4]	0.455[−4]	0.4145[−4]	0.454[−5]	0.420[−5]	0.391[−5]	0.3716[−5]
3	0.1[−1]	0.542[−3]	0.340[−3]	0.448[−3]	0.4090[−3]	0.445[−4]	0.362[−4]	0.384[−4]	0.3659[−4]
3	0.1	0.457[−2]	0.292[−2]	0.389[−2]	0.3622[−2]	0.375[−3]	0.307[−3]	0.330[−3]	0.3183[−3]
3	1	0.200[−1]	0.142[−1]	0.180[−1]	0.1764[−1]	0.164[−2]	0.141[−2]	0.149[−2]	0.1480[−2]
3	10	0.337[−1]	0.278[−1]	0.309[−1]	0.3055[−1]	0.276[−2]	0.252[−2]	0.254[−2]	0.2529[−2]
3	100	0.366[−1]	0.311[−1]	0.336[−1]	0.3321[−1]	0.300[−2]	0.278[−2]	0.276[−2]	0.2748[−2]

It is straightforward to construct the matrix representation of the Hamiltonian (40) in the basis (41). One obtains

$$\begin{aligned} H_{\mathbf{n}m,\mathbf{n}'m'} = &\left[\mu_m + \sum_{i=1}^{N} (1+\varepsilon_i)\gamma_i n_i\right]\delta_{\mathbf{n},\mathbf{n}'}\delta_{m,m'} \\ &+ R_{m',m}\sum_{i=1}^{N} \sqrt{\gamma_i D(n_i'+1)}\,\delta_{n_i,n_i'+1}\delta^{i}_{\mathbf{n},\mathbf{n}'} \\ &+ R_{m,m'}\sum_{i=1}^{N} \sqrt{\gamma_i D n_i'}\,\delta_{n_i,n_i'-1}\delta^{i}_{\mathbf{n},\mathbf{n}'} \\ &+ \frac{1}{2}\delta_{m,m'}\sum_{i=1}^{N}\sum_{j\neq i}^{N} \sqrt{\gamma_i\gamma_j}\,[\sqrt{n_i'(n_j'+1)} \\ &\times \delta_{n_i,n_i'-1}\delta_{n_j,n_j'+1} \\ &+ \sqrt{(n_i'+1)n_j'}\,\delta_{n_i,n_i'+1}\delta_{n_j,n_j'-1}]\delta^{i,j}_{\mathbf{n},\mathbf{n}'}, \end{aligned} \tag{44}$$

$$\delta^{i}_{\mathbf{n},\mathbf{n}'} = \prod_{k\neq i}\delta_{n_k,n_k'}, \quad \delta^{i,j}_{\mathbf{n},\mathbf{n}'} = \prod_{k\neq i,j}\delta_{n_k,n_k'},$$

where

$$R_{m,m'} = \langle m|e^{U/2D}\partial_x g' e^{-U/2D}|m'\rangle. \tag{45}$$

In the present case of a single bath mode, it reads

$$\begin{aligned} H_{nm,n'm'} = &[\mu_m + (1+\varepsilon)\gamma n]\delta_{n,n'}\delta_{m,m'} \\ &+ \sqrt{\gamma D(n'+1)}\,\delta_{n,n'+1}R_{m',m} \\ &+ \sqrt{\gamma D n'}\,\delta_{n,n'-1}R_{m,m'}. \end{aligned} \tag{46}$$

This representation has the advantage that a few basis functions are sufficient to produce very accurate low-lying eigenvalues for $\varepsilon \geq 1$. The method is rather *insensitive* with respect to the barrier height and the coupling constant. With a decreasing anisotropy parameter the convergence only slowly becomes worse. Even for $\varepsilon < e^{-E}$ a number of 10–15

basis functions per x and y are typically required regardless of the coupling constant. The resulting matrices can be diagonalized by standard routines for sparse or band structured matrices.

Now, it remains to evaluate the eigenvalues μ_m and the matrix elements $R_{m,m'}$. For this purpose we use a complete orthonormal set of functions $|i\rangle$, i.e.,

$$\chi_m=\sum_{i=0}^{\infty} C_{m,i}|i\rangle, \tag{47}$$

that are eigenfunctions of the *scaled* harmonic oscillator

$$\left(-D\partial_{xx}^2+\frac{\omega^2}{4D}x^2-\frac{\omega}{2}\right)|i\rangle=\omega i|i\rangle, \tag{48}$$

where the frequency ω is a free parameter that can be chosen such that the convergence of the series in (47) is as fast as possible. Both the matrix representation of the Hamiltonian (43) and the method for determining ω are given in the Appendix. Here we only note that the use of the basis of scaled harmonic oscillator eigenfunctions allows one to truncate the sum in (47) at least at half of the number of terms that are necessary to converge to 12 significant digits compared to the standard unscaled basis corresponding to $\omega=1$. Another advantage of the basis (48) is that the matrix elements $R_{m,m'}$ can be evaluated *analytically*, that is, without loss of accuracy. For the potential $U(x)$ defined by (5) a straightforward calculation yields the algebraic expression

$$\begin{aligned}R_{n,m}=&\sum_{i=0}^{M-1}\sqrt{i+1}\left\{\sqrt{\frac{D}{4\omega}}\left[\frac{3D}{\omega}(i+1)-1\right]\right.\\&\times(C_{n,i}C_{m,i+1}+C_{n,i+1}C_{m,i})\\&\left.-\sqrt{\frac{\omega}{4D}}(C_{n,i}C_{m,i+1}-C_{n,i+1}C_{m,i})\right\}\\&+\frac{(D/\omega)^{3/2}}{2D}\sum_{i=0}^{M-3}\sqrt{(i+1)(i+2)(i+3)}\\&\times(C_{n,i+3}C_{m,i}+C_{n,i}C_{m,i+3}).\end{aligned} \tag{49}$$

IV. RESULTS

The least nonvanishing eigenvalue and the corresponding eigenfunction of the two-dimensional Smoluchowski equation (5) have been calculated in a wide range of parameters. The results for the eigenvalue are presented in Tables I and II and compared to the Langer formula (23), the full Rayleigh quotient (27), and its asymptotic value including the first-order corrections in the inverse barrier height $D/4=E^{-1}$ (29). As for $E\geqslant 5$, the inequalities $0.99\leqslant N_0<1$ usually hold; we have set $N_0=1$ in evaluating the full Rayleigh quotient (27) for $E=5$, 7.5, and 10.

For large parameters ε, γ, and E, all approximate rate expressions agree well with the numerically exact least nonvanishing eigenvalue λ. Large deviations are found if both ε and γ are small. The region of complete failure of all approximate expressions grows slowly towards larger ε and γ values with decreasing barrier height. For barrier heights smaller than $E=5$, the dependence of the denominator (Q,Q) of the Rayleigh quotient on the detailed shape of the trial function $Q(x,y)$ must be taken into account. In particular, the factor N_0 in the denominator of (27) must not be approximated by unity. Table III gives the scalar product N_0 for $E=2.5$ and various values of ε and γ. Though the resulting corrections are ''exponentially small'' they do not much differ in magnitude from the ''leading'' algebraic corrections for low barrier heights. This indicates that the rate description as a whole loses its meaning for too low barriers. It is interesting to note that this failure may be due to the equilibrium properties of the system. The equilibrium distribution (9) no longer allows an unambiguous definition of the populations of the different metastable states [20,25] although the long-time dynamics may still be governed by a single least nonvanishing eigenvalue that is well separated from the rest of the finite eigenvalues [13].

For the parameter values that are used in Tables I and II, the Kramers-Langer expression has its minimal error of about 4% for $E=10$ and $\varepsilon\geqslant 10$ for all values of γ. The error increases with decreasing ε for all values of γ, but is strongest for small γ. For $E=10$ it completely fails for $\gamma<1.5$ and $\varepsilon<0.1$. For small values of ε the error of the Kramers-Langer rate decreases only rather slowly with increasing γ. Finite-barrier corrections according to (29) lead to a considerable improvement in many cases. For $E=10$ and $\gamma\geqslant 2$ already the leading finite-barrier corrections agree very well with the exact rates. If, however, the condition $\alpha^2 D<0.1$ is violated, the corrections in (29) are not sufficient and (29) may yield even negative results. These instances are indicated by bars in Tables I and II. Finite-barrier corrections must then be determined by means of the full Rayleigh quotient (27) including N_0 for $E<5$, in which case N_0 cannot be approximated by unity. For $E=10$ and $\varepsilon>0.1$ Eq. (27) gives excellent results for all considered values of γ. If, however, $\gamma\leqslant 1$ and $\varepsilon\leqslant 0.01$, all approximate rate expressions, including (27), strongly deviate by factors, or even by orders of magnitude, from the numerically exact least nonvanishing eigenvalue.

Note that the Kramers-Langer rate is always larger than the Rayleigh quotient. Both λ_{KL} and $\lambda^{(1)}$ are larger than the numerically exact least nonvanishing eigenvalue as one expects. This bounding property, however, does not hold for $N_0\lambda^{(1)}$, that is, if one sets, in (27), $N_0=1$. This is seen from Table III, in which the product $N_0\lambda^{(1)}$ is shown and compared with the numerically exact results for $E=2.5$.

The relative errors of the different approximations are displayed in Fig. 2 as functions of ε for various values of E and γ. The relative deviation of the Kramers-Langer rate from the Rayleigh quotient reading

$$\vartheta=\frac{\lambda_{\mathrm{KL}}-\lambda^{(1)}}{\lambda^{(1)}}\times 100\% \tag{50}$$

yields a simple self-consistent criterion for the trial function (19). If $Q(x,y)$ had been an exact eigenfunction, the Kramers-Langer rate and the Rayleigh quotient would coincide. Figure 3 displays the curves of constant ϑ in the ε-γ plane for different values of E. The lines corresponding to $\vartheta=20\%$ reach their maximal values of ε at $\gamma<1$. The branches on the right-hand side of the maxima represent a

TABLE II. Same as in Table I, but for $E=7.5$ and 10.

		$E=7.5$				$E=10$			
γ	ε	λ_{KL}	λ_{RQ}	$N_0\lambda^{(1)}$	λ	λ_{KL}	λ_{RQ}	$N_0\lambda^{(1)}$	λ
0.5	0.1[−2]	0.125[−3]	0.118[−3]	0.106[−3]	0.2958[−5]	0.102[−4]	0.831[−5]	0.901[−5]	0.5224[−6]
0.5	0.1[−1]	0.126[−3]	0.944[−4]	0.107[−3]	0.2320[−4]	0.103[−4]	0.839[−5]	0.912[−5]	0.3227[−5]
0.5	0.1	0.135[−3]	0.103[−3]	0.118[−3]	0.8816[−4]	0.111[−4]	0.910[−5]	0.100[−4]	0.8473[−5]
0.5	1	0.176[−3]	0.145[−3]	0.163[−3]	0.1601[−3]	0.145[−4]	0.126[−4]	0.136[−4]	0.1352[−4]
0.5	10	0.230[−3]	0.212[−3]	0.217[−3]	0.2161[−3]	0.188[−4]	0.178[−4]	0.180[−4]	0.1804[−4]
0.5	100	0.247[−3]	0.234[−3]	0.233[−3]	0.2324[−3]	0.202[−4]	0.195[−4]	0.194[−4]	0.1939[−4]
1	0.1[−2]	0.775[−5]	0.736[−5]	0.302[−5]	0.7839[−6]	0.636[−6]		0.266[−6]	0.7848[−7]
1	0.1[−1]	0.237[−4]		0.146[−4]	0.7340[−5]	0.194[−5]		0.127[−5]	0.7184[−6]
1	0.1	0.673[−4]		0.565[−4]	0.4798[−4]	0.552[−5]		0.479[−5]	0.4301[−5]
1	1	0.154[−3]	0.109[−3]	0.143[−3]	0.1414[−3]	0.126[−4]	0.985[−5]	0.119[−4]	0.1189[−4]
1	10	0.228[−3]	0.212[−3]	0.216[−3]	0.2148[−3]	0.187[−4]	0.177[−4]	0.179[−4]	0.1793[−4]
1	100	0.247[−3]	0.234[−3]	0.233[−3]	0.2324[−3]	0.202[−4]	0.195[−4]	0.194[−4]	0.1939[−4]
1.5	0.1[−2]	0.740[−6]	0.703[−6]	0.569[−6]	0.4893[−6]	0.608[−7]	0.319[−7]	0.488[−7]	0.4379[−7]
1.5	0.1[−1]	0.688[−5]	0.253[−5]	0.543[−5]	0.4732[−5]	0.565[−6]	0.348[−6]	0.464[−6]	0.4215[−6]
1.5	0.1	0.450[−4]	0.220[−4]	0.392[−4]	0.3651[−4]	0.369[−5]	0.315[−5]	0.331[−5]	0.3164[−5]
1.5	1	0.145[−3]	0.116[−3]	0.135[−3]	0.1339[−3]	0.119[−4]	0.113[−4]	0.113[−4]	0.1123[−4]
1.5	10	0.228[−3]	0.213[−3]	0.215[−3]	0.2143[−3]	0.187[−4]	0.180[−4]	0.179[−4]	0.1789[−4]
1.5	100	0.247[−3]	0.234[−3]	0.233[−3]	0.2324[−3]	0.202[−4]	0.195[−4]	0.194[−4]	0.1939[−4]
2	0.1[−2]	0.496[−6]	0.471[−6]	0.423[−6]	0.3955[−6]	0.407[−7]	0.331[−7]	0.358[−7]	0.3431[−7]
2	0.1[−1]	0.479[−5]	0.360[−5]	0.412[−5]	0.3864[−5]	0.393[−6]	0.320[−6]	0.348[−6]	0.3345[−6]
2	0.1	0.369[−4]	0.285[−4]	0.330[−4]	0.3173[−4]	0.303[−5]	0.251[−5]	0.278[−5]	0.2712[−5]
2	1	0.140[−3]	0.120[−3]	0.131[−3]	0.1299[−3]	0.115[−4]	0.103[−4]	0.109[−4]	0.1089[−4]
2	10	0.227[−3]	0.213[−3]	0.215[−3]	0.2141[−3]	0.187[−4]	0.178[−4]	0.179[−4]	0.1787[−4]
2	100	0.247[−3]	0.234[−3]	0.233[−3]	0.2324[−3]	0.202[−4]	0.195[−4]	0.194[−4]	0.1939[−4]
3	0.1[−2]	0.373[−6]	0.354[−6]	0.336[−6]	0.3260[−6]	0.306[−7]	0.277[−7]	0.282[−7]	0.2773[−7]
3	0.1[−1]	0.365[−5]	0.320[−5]	0.330[−5]	0.3206[−5]	0.300[−6]	0.273[−6]	0.277[−6]	0.2725[−6]
3	0.1	0.308[−4]	0.271[−4]	0.282[−4]	0.2764[−4]	0.253[−5]	0.235[−5]	0.236[−5]	0.2337[−5]
3	1	0.135[−3]	0.122[−3]	0.126[−3]	0.1258[−3]	0.111[−4]	0.106[−4]	0.105[−4]	0.1053[−4]
3	10	0.227[−3]	0.214[−3]	0.215[−3]	0.2139[−3]	0.186[−4]	0.179[−4]	0.178[−4]	0.1785[−4]
3	100	0.247[−3]	0.234[−3]	0.233[−3]	0.2324[−3]	0.202[−4]	0.195[−4]	0.194[−4]	0.1939[−4]

reliable border line of applicability of the Kramers-Langer theory and the Rayleigh quotient based on the trial function (19). For values on the left-hand side of the maximum the criterion fails since the true eigenfunction differs too much from the trial function (19).

Figure 4 shows numerical results for the eigenfunction $Q(x,y)$ and its node line, which coincides with the stochastic separatrix. We find that $Q(x,y)$ and consequently also the stochastic separatrix rotates with decreasing anisotropy parameter. It moves in a counterclockwise direction from the y axis for large ε to the x axis in the strongly anisotropic limit $\varepsilon\to 0$ for all values of the coupling constant. This is in contrast to the behavior of the deterministic separatrix (37), which does not approach the x axis if $\gamma<1$. Hence we conclude that a reason for the failure of the Kramers-Langer theory is the different location of the stochastic and deterministic separatrix for small values of ε.

In Fig. 5 the stochastic and the deterministic separatrices are compared for different parameter values. They are indistinguishable from each other for all ε if the coupling between the system and the nonreactive mode is sufficiently strong, i.e., $\gamma\geqslant U''(x_{\min})=2$. This is not the case for $\gamma<2$. Then the difference between the stochastic and the deterministic separatrix, which is still invisible for $\varepsilon\geqslant 10$, increases with decreasing anisotropy parameter. Figure 6 shows that the stochastic separatrix $y_{SS}(x)$ becomes curved for $\varepsilon\leqslant 1$ and has a slope at $x=y=0$ that is different from that of $y_{DS}(x)$. One also sees that the finite-barrier expansion for the stochastic separatrix (36) accounts quantitatively for this difference. Finally, with further decreasing ε, the slope of the deterministic separatrix approaches a finite limiting value, namely, $w=\gamma^{-1}-1$, in contrast to the stochastic separatrix. All these peculiarities become more evident for smaller values of γ (see Fig. 7). For $\gamma<0.5$ the Kramers-Langer function becomes inapplicable already for $\varepsilon\approx 1$.

Besides the location of the node line, the shape of the trial function perpendicular to the node line is another important factor that influences the value of the Rayleigh quotient. Using $z=(wx+y)/(w^2+1)^{1/2}$ as a coordinate in the direction transverse to the node, one obtains as the profile of the Kramers-Langer function

$$Q_{(0)}(z)=\sqrt{\frac{2}{\pi\sigma^2}}\int_0^z du\,\exp\left\{-\frac{u^2}{2\sigma^2}\right\}, \tag{51}$$

where the width reads

$$\sigma=[b(w^2+1)]^{-1/2}. \tag{52}$$

TABLE III. Scalar product $N_0=(Q_{(0)},Q_{(0)})$, as well as a comparison between the Rayleigh quotient [Eq. (27)] evaluated with $N_0=1$, $N_0\lambda^{(1)}$, and the numerically exact results λ for the least nonvanishing eigenvalue of the Smoluchowski operator (5) for $E=2.5$.

γ	ε	N_0	$N_0\lambda^{(1)}$	λ
0.5	0.1[−2]	0.92	0.130[−1]	0.6929[−4]
0.5	0.1[−1]	0.92	0.132[−1]	0.6768[−3]
0.5	0.1	0.91	0.148[−1]	0.5529[−2]
0.5	1	0.90	0.213[−1]	0.2046[−1]
0.5	10	0.89	0.288[−1]	0.3078[−1]
0.5	100	0.89	0.310[−1]	0.3321[−1]
1	0.1[−2]	0.96	0.323[−3]	0.5686[−4]
1	0.1[−1]	0.95	0.164[−2]	0.5567[−3]
1	0.1	0.93	0.686[−2]	0.4648[−2]
1	1	0.92	0.187[−1]	0.1904[−1]
1	10	0.91	0.287[−1]	0.3065[−1]
1	100	0.91	0.310[−1]	0.3321[−1]
1.5	0.1[−2]	0.94	0.668[−4]	0.4963[−4]
1.5	0.1[−1]	0.94	0.644[−3]	0.4876[−3]
1.5	0.1	0.93	0.485[−2]	0.4173[−2]
1.5	1	0.92	0.177[−1]	0.1839[−1]
1.5	10	0.91	0.286[−1]	0.3060[−1]
1.5	100	0.91	0.310[−1]	0.3321[−1]
2	0.1[−2]	0.93	0.519[−4]	0.4559[−4]
2	0.1[−1]	0.93	0.507[−3]	0.4489[−3]
2	0.1	0.93	0.417[−2]	0.3905[−2]
2	1	0.92	0.172[−1]	0.1803[−1]
2	10	0.92	0.286[−1]	0.3057[−1]
2	100	0.91	0.310[−1]	0.3321[−1]
3	0.1[−2]	0.93	0.426[−4]	0.4145[−4]
3	0.1[−1]	0.93	0.420[−3]	0.4090[−3]
3	0.1	0.93	0.363[−2]	0.3622[−2]
3	1	0.92	0.167[−1]	0.1764[−1]
3	10	0.92	0.286[−1]	0.3055[−1]
3	100	0.92	0.310[−1]	0.3321[−1]

Here b and w are given by (20) and (21), respectively. The width σ is a function of ε and γ, which tends to unity in the limit $\varepsilon\to\infty$ for all coupling constants. For ε going to zero, the width approaches a finite value for all γ except $\gamma=1$, where σ vanishes. Since w simultaneously vanishes, the trial function (19) becomes a step function jumping at $y=0$:

$$Q_{(0)}(x,y)=\begin{cases}1 & \text{if } y>0\\ 0 & \text{if } y=0\\ -1 & \text{otherwise.}\end{cases} \tag{53}$$

However, the numerically exact eigenfunctions do not show this behavior. They rather keep a finite width for all coupling strengths in the strongly anisotropic limit. For $\gamma>1$ and all ε the profile is in qualitative agreement with that of the Kramers-Langer function (51). The first-order correction (34) quantitatively agrees with the numerical results.

Figure 8 shows a comparison of the profiles of the numerically exact eigenfunction $Q(x,y)$, the Kramers-Langer function (19), and the perturbation expansion (34). It is interesting that the shape of the true eigenfunction agrees quite well with an error function even for $\gamma<1$ and $\varepsilon\to0$, i.e., also in cases when both the Kramers-Langer rate λ_{KL} and the Rayleigh quotient $\lambda^{(1)}$ fail grossly. Figure 9 shows that in this case, the profile of $Q(x,y)$ coincides surprisingly well with that given by (51) though the stochastic and the deterministic separatrices differ very much [see Fig. 6(c)]. Thus one can conclude that if the coupling is not too weak $0.5\leqslant\gamma<1$, the main reason for the breakdown of the Kramers-Langer theory is the different location of the deterministic and stochastic separatrices in the strongly anisotropic limit and their different respective slopes at the saddle

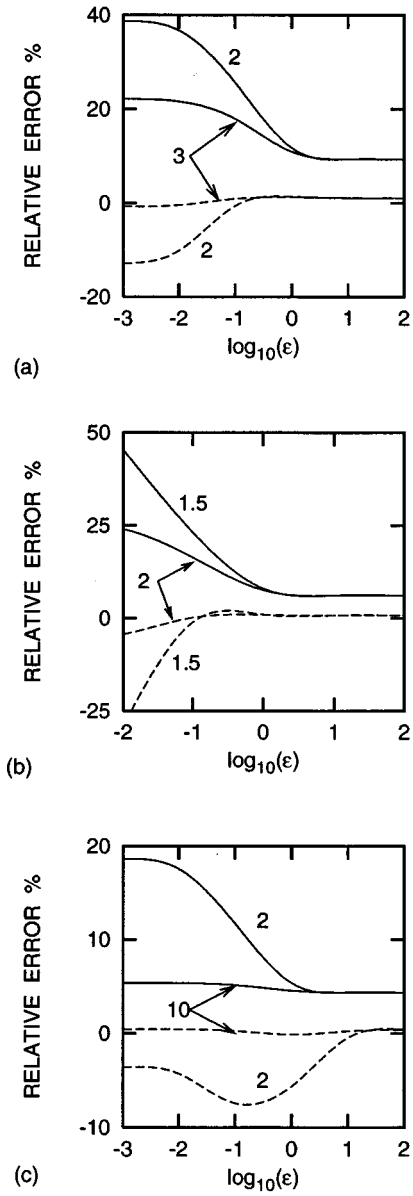

FIG. 2. Relative errors, 100% [(approximate) − (exact)/(exact)], for the different approximate expressions for the least nonvanishing eigenvalue. The solid and the dashed lines show the errors of the Kramers-Langer formula [Eq. (23)] and of the Rayleigh quotient [Eq. (29)] including the first-order corrections, respectively. (a) $E=5$ and $\gamma=2,3$; (b) $E=7.5$ and $\gamma=1.5,2$; (c) $E=10$ and $\gamma=2,10$.

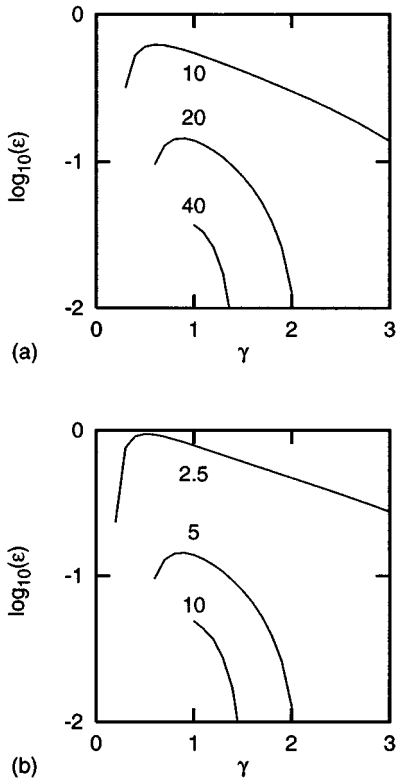

FIG. 3. Border lines [Eq. (50)] of applicability of the Kramers-Langer theory as a function of ε and γ. (a) $E=5$ and $\vartheta=10,20,40$; (b) $\vartheta=20$ and $E=2.5,5,10$.

point of the potential. Only in the limit of weak coupling $\gamma\rightarrow 0$ is the shape of the true eigenfunction seen to be quite different from an error function following from the Kramers-Langer theory [see Fig. 9(b)]. As we showed in another paper [13], with γ going to zero the spectrum of eigenvalues of

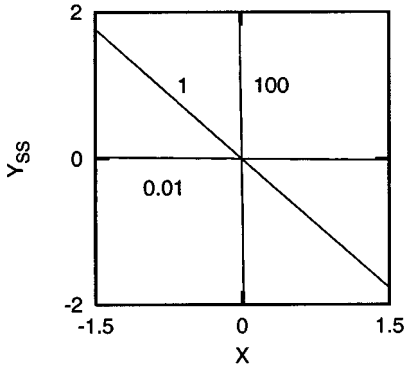

FIG. 5. Location of the stochastic separatrix in the vicinity of the saddle point for $E=5$, $\gamma=3$, and $\varepsilon=0.01,1,100$.

the Smoluchowski operator becomes very similar to that of the harmonic oscillator even though $\varepsilon>1$, and therefore the rate description is inapplicable in this case.

V. CONCLUSION

In this paper we discussed the validity of the Kramers-Langer theory by a comparison with numerical results for the least nonvanishing eigenvalue and the corresponding eigenfunction. The investigation was performed for a reactive mode that is coupled to a relaxation mode and a heat bath. The dynamics of both modes are strongly damped such that inertial effects can safely be neglected and a two-dimensional Smoluchowski equation describes the process. Yet the relaxation times of the reactive and the relaxational modes may differ, leading to an anisotropy in the respective diffusion constants. Depending on the ratio of the diffusion constants, i.e., the anisotropy parameter ε, the coupling constant γ of the two modes, and the dimensionless temperature D of the heat bath, the system belongs to either the relax-

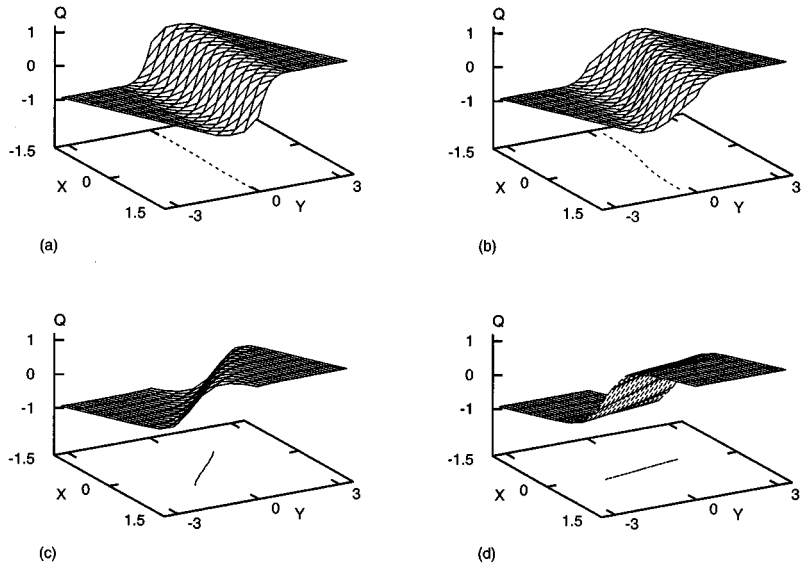

FIG. 4. Eigenfunction $Q(x,y)$ corresponding to the least nonvanishing eigenvalue λ_1 for $E=5$ and $\gamma=0.5$. (a) $\varepsilon=10$; (b) $\varepsilon=1$; (c) $\varepsilon=0.1$; (d) $\varepsilon=0.01$.

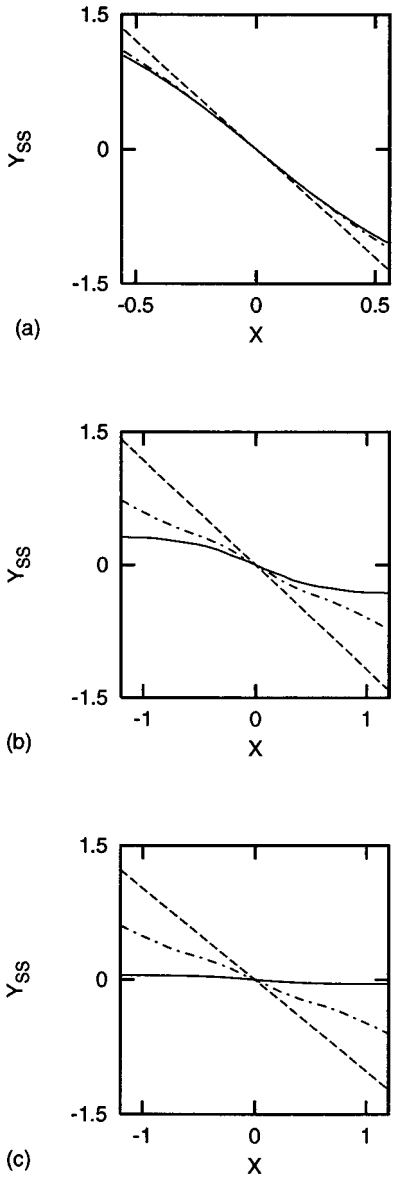

FIG. 6. Location of the stochastic separatrix for $E=5$ and $\gamma=0.5$. The solid and the dashed lines represent the numerically exact results and the deterministic separatrix [Eq. (37)], respectively. The dot-dashed lines show the perturbation expansion [Eqs. (34) and (35)]. (a) $\varepsilon=1$; (b) $\varepsilon=0.1$; (c) $\varepsilon=0.01$.

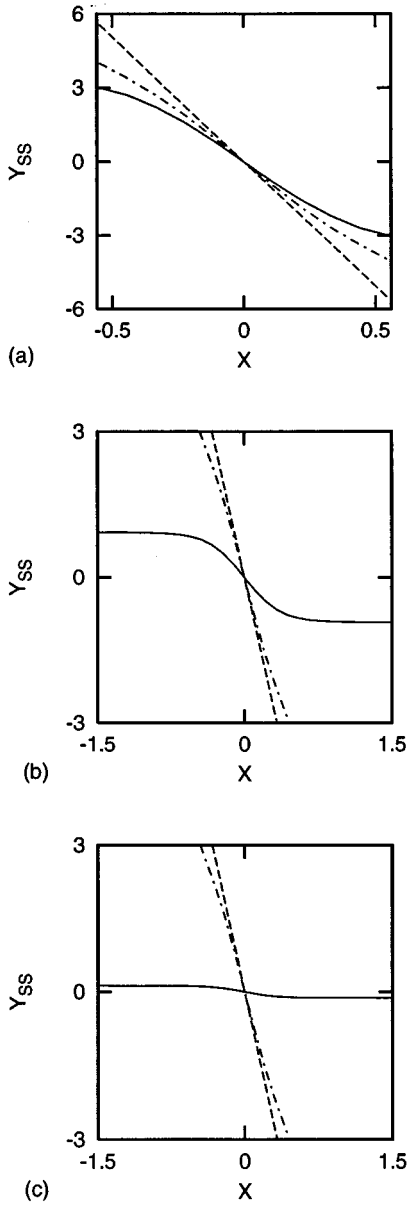

FIG. 7. Same as in Fig. 6, but for $\gamma=0.1$.

ational or the rate regime. The latter can further be subdivided into the anisotropic and the Kramers-Langer regime.

The relaxational regime is characterized by a small coupling constant γ such that the reactive and the relaxational modes are almost decoupled. The long-time behavior in this regime is determined by a set of approximately equally spaced low-lying eigenvalues. On the contrary, at larger values of γ, i.e., in the two other regimes, the long-time behavior is determined by the barrier crossing process leading to a least nonvanishing eigenvalue that is separated from all larger ones by an exponentially large gap. The precise location of the crossover between the relaxational regime and the rate regime as a function of D, ε, and γ has not yet been investigated systematically. Results from [13] clearly indicate that for fixed D the critical value of γ where the crossover takes place decreases with increasing ε. Since the transition rate characterizing the barrier crossing process and hence the corresponding eigenvalue is exponentially small in the inverse temperature D, the critical value of γ must also be exponentially small in D.

The Kramers-Langer regime extends to large values of ε and γ. Hence D is the relevant small parameter in the Kramers-Langer regime. In this whole regime, the least nonvanishing eigenvalue is determined by the Kramers-Langer rate formula (23). Possible deviations come from finite-barrier corrections and can be accounted for by the Rayleigh quotient $\lambda^{(1)}$ [see Eq. (27)], which is based on the unperturbed Kramers function $Q_{(0)}(x,y)$ given in (19) as a trial function. A further improvement of the eigenvalue, namely, up to the order of the third power of the inverse barrier height, can be obtained when the Rayleigh quotient is evaluated with the improved eigenfunction $Q_{(0)}(x,y)$

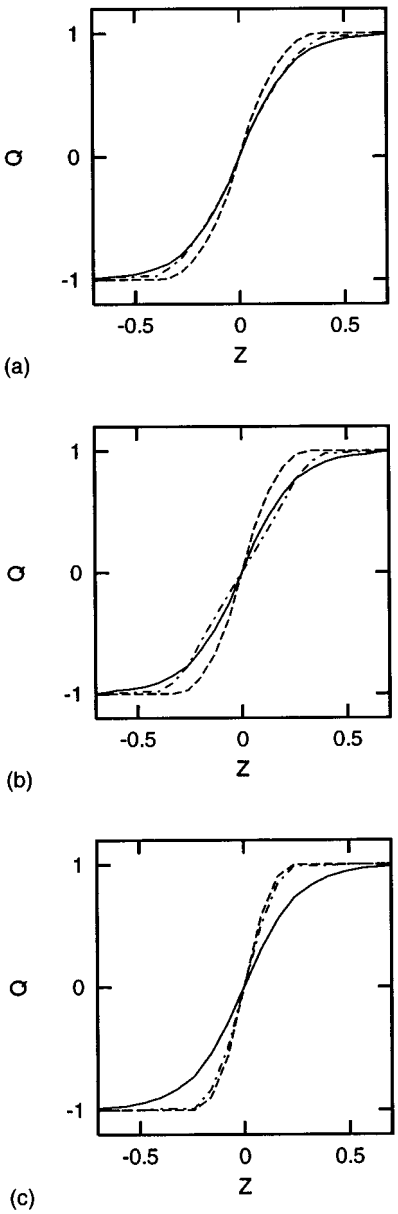

FIG. 8. Profiles of the eigenfunction $Q(x,y)$ for $E=5$ and $\varepsilon=0.01$. The solid lines show the numerically exact results. The dashed and the dot-dashed lines show the Kramers-Langer function [Eq. (19)] and the perturbation expansion [Eq. (34)], respectively. (a) $\gamma=2$; (b) $\gamma=1.5$; (c) $\gamma=1$.

$+Q_{(1)}(x,y)$ given by (19) and (31). However, we did not consider this here.

Using a self-consistent criterion, we correctly predicted the transition regime where the Kramers-Langer theory loses its validity and the anisotropy regime is reached when the coupling constant is decreased at a sufficiently small value of ε. The criterion is not reliable at yet smaller values of γ, where it indicates a spurious recovery of the Kramers-Langer theory. Within the transition regime the Rayleigh quotient with the Kramers-Langer trial function still gives a reliable value for the least nonvanishing eigenvalue. This is no longer the case for parameter values within the anisotropic regime.

Corrected eigenfunctions were obtained by means of a

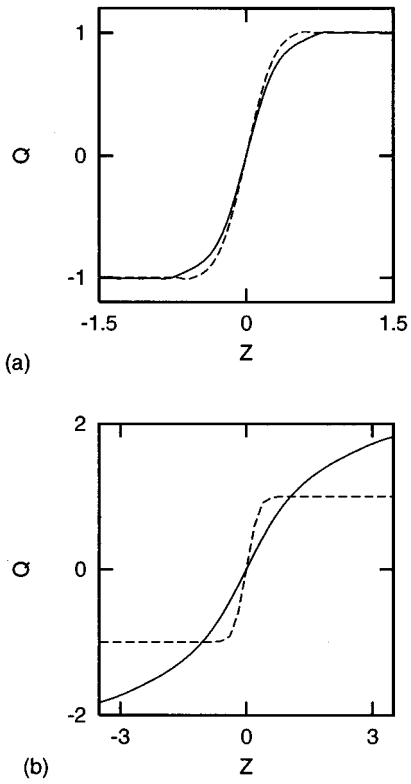

FIG. 9. Same as in Fig. 8, but for $\gamma<1$. (a) $\gamma=0.5$; (b) $\gamma=0.1$.

perturbation theory about the unperturbed case of a harmonic barrier. They have a curved node line that is rotated relative to the node of the unperturbed Kramers function. Both the rotation and the curvature quantitatively describe the difference between the stochastic and the deterministic separatrix both in the Kramers-Langer and the transition regime.

Yet another important feature is the form of the eigenfunction transversal to its node. From the result of the first-order perturbation theory one finds that this form can be written as an error function. It is interesting to note that the numerically exact eigenfunctions show the error function profile in quite a large region of parameter values, even deeply inside the anisotropic regime where the Kramers-Langer theory and also the perturbation theory completely fail. This observation suggests a simple ansatz for the eigenfunction belonging to the least nonvanishing eigenvalue reading

$$Q(x,y)=\sqrt{\frac{2}{\pi}}\int_0^{ax+cy} du\,\exp\left\{-\frac{1}{2}u^2\right\}, \tag{54}$$

where a and c are free parameters that have to be chosen such that the Rayleigh quotient is minimal. In this way we expect to obtain good results for the least nonvanishing eigenvalue, except for a too low temperature, in which case the ansatz has to be modified by taking into account the curvature of the stochastic separatrix. In the relaxational regime, where γ is extremely small, we also do not expect (54) to hold. There a polynomial in y seems to be a more appropriate ansatz for the trial function.

ACKNOWLEDGMENTS

We thank Alexander Berezhkovskii and Vladick Zitserman for many stimulating discussions and are grateful to Jens Emmerich for his help with various numerical problems. This work was supported by Schweizerischer Nationalfond.

APPENDIX

The aim of this Appendix is to give the matrix representation of the Hamiltonian (43) in the basis (48) and further to show a way of determining the free parameter ω. For notational simplicity we rewrite the problem in the form

$$(-\partial_{xx}^2+v_0+v_2x^2+v_4x^4+v_6x^6)\chi_m=E_m\chi_m, \quad \text{(A1)}$$

$$\left(-\partial_{xx}^2+\frac{\Omega^2}{4}x^2-\frac{\Omega}{2}\right)|i\rangle=\Omega i|i\rangle,$$

where $E_m=\mu_m/D$ and $\Omega=\omega/D$, while the coefficients v_m of the Schrödinger potential are determined by those of $U(x)$ and D, reading

$$v_0=\frac{1}{2D}, \quad v_2=\frac{1}{4D^2}-\frac{3}{2D}, \quad v_4=-\frac{1}{2D^2}, \quad v_6=\frac{1}{4D^2}.$$

The matrix representation of (A1) in the basis $|i\rangle$ can be found easily if one uses the well-known relationships of harmonic-oscillator eigenfunctions

$$\langle i|j\rangle=\delta_{i,j},$$

$$x|i\rangle=\frac{1}{\sqrt{\Omega}}[\sqrt{i}|i-1\rangle+\sqrt{i+1}|i+1\rangle],$$

$$\partial_x|i\rangle=\frac{1}{2}\sqrt{\Omega}[\sqrt{i}|i-1\rangle-\sqrt{i+1}|i+1\rangle]. \quad \text{(A2)}$$

The resulting matrix has a band structure, where the diagonals are given by

$$H_{n,n}=v_0+\left(\frac{\Omega}{4}+\frac{v_2}{\Omega}\right)(1+2n)+\frac{3v_4}{\Omega^2}(1+2n+2n^2)+\frac{5v_6}{\Omega^3}(3+8n+6n^2+4n^3), \quad \text{(A3)}$$

$$H_{n,n-2}=H_{n-2,n}=\sqrt{n(n-1)}\left[-\frac{\Omega}{4}+\frac{v_2}{\Omega}+\frac{2v_4}{\Omega^2}(2n-1)+\frac{15v_6}{\Omega^3}(1-n+n^2)\right],$$

$$H_{n,n-4}=H_{n-4,n}=\sqrt{n(n-1)(n-2)(n-3)}\times\left[\frac{v_4}{\Omega^2}+\frac{3v_6}{\Omega^3}(2n-3)\right],$$

$$H_{n,n-6}=H_{n-6,n}=\frac{v_6}{\Omega^3}[n(n-1)(n-2)(n-3)\times(n-4)(n-5)]^{1/2},$$

while the remaining matrix elements are equal to zero.

It is clear that neither E_m nor χ_m is a function of Ω. As we are unable, however, to handle the infinite expansion in (48), we have to truncate it at some finite $i=M-1$. Then the resulting approximations E_m^M and χ_m^M of the eigenfunctions and eigenvalues depend on Ω. However, the parameter Ω can be optimized to yield good approximations of the eigenvalues and eigenfunctions. The upper bound property of the Rayleigh-Ritz method yields the following inequality for the sum of the true and approximated eigenvalues:

$$\sum_{m=0}^{M-1}E_m\leqslant\sum_{m=0}^{M-1}E_m^M=\sum_{m=0}^{M-1}H_{m,m}. \quad \text{(A4)}$$

Thus minimizing the trace of the Hamiltonian operator in the basis of scaled harmonic-oscillator eigenfunctions provides one with a minimal average error of the eigenvalues E_M^m and, consequently, a reasonable choice of the free parameter for a given number of basis function M. When applied to (A3), this yields, after some lengthy but simple algebra, a polynomial of the form [26]

$$\Omega^4-4v_2\Omega^2-8v_4(2M+1/M)\Omega-60v_6(M^2+2)=0, \quad \text{(A5)}$$

which is easily solved for Ω when M is large:

$$\Omega=(60v_6M^2)^{1/4}. \quad \text{(A6)}$$

Returning in (A6) to the original notation, one immediately obtains

$$\omega=(15D^2M^2)^{1/4}. \quad \text{(A7)}$$

[1] H.A. Kramers, Physica **7**, 284 (1940).

[2] For recent reviews, see B.J. Berne, M. Borkovec, and J.E. Straub, J. Phys. Chem. **92**, 3711 (1988); P. Hänggi, P. Talkner, and M. Borkovec, Rev. Mod. Phys. **62**, 251 (1990); V.I. Mel'nikov, Phys. Rep. **209**, 1 (1991); *Activated Barrier Crossing*, edited by P. Hänggi and G. Fleming (World Scientific, Singapore, 1992); *New Trends in Kramers' Reaction Rate Theory*, edited by P. Talkner and P. Hänggi (Kluwer Academic, Dordrecht, 1995).

[3] H.C. Brinkman, Physica **22**, 149 (1956); R. Landauer and J.A. Swanson, Phys. Rev. **121**, 1668 (1961).

[4] J.S. Langer, Ann. Phys. (N.Y.) **54**, 258 (1969).

[5] P. Talkner, Z. Phys. B **68**, 201 (1987).

[6] A.N. Drozdov, Physica A **187**, 329 (1992).

[7] R.F. Grote and J.T. Hynes, J. Chem. Phys. **73**, 2715 (1980); P. Hänggi and F. Mojtabai, Phys. Rev. A **26**, 1168 (1982); H. Grabert, Phys. Rev. Lett. **61**, 1683 (1988); E. Pollak, H. Grabert, and P. Hänggi, J. Chem. Phys. **91**, 4073 (1989); R. Graham, J. Stat. Phys. **60**, 473 (1990).

[8] P. Talkner and H.B. Braun, J. Chem. Phys. **88**, 7537 (1988).

[9] B. Carmeli and A. Nitzan, Phys. Rev. Lett. **49**, 423 (1982).
[10] E. Pollak and E. Hershkowits, Chem. Phys. **180**, 191 (1994).
[11] J.E. Straub, M. Borkovec, and B.J. Berne, J. Chem. Phys. **83**, 3172 (1985); **84**, 1788 (1986); **86**, 4296 (1987).
[12] A.M. Berezhkovskii, Chem. Phys. **164**, 331 (1992).
[13] A.N. Drozdov and P. Talkner, J. Chem. Phys. **105**, 4117 (1996).
[14] A.M. Berezhkovskii and V.Yu. Zitserman, Chem. Phys. Lett. **158**, 369 (1989); J. Phys. A **25**, 2077 (1992); Physica A **187**, 519 (1992); Chem. Phys. **164**, 331 (1992).
[15] N. Agmon and S. Rabinovich, J. Chem. Phys. **97**, 7270 (1992).
[16] M.M. Kłosek-Dygas, B.M. Hoffman, B.J. Matkowsky, A. Nitzan, M.A Ratner, and Z. Schuss, J. Chem. Phys. **90**, 1141 (1989).
[17] A.M. Berezhkovskii, E. Pollak, and V.Yu. Zitserman, J. Chem. Phys. **97**, 2422 (1992); A.M. Berezhkovskii, A.M. Frishman, and E. Pollak, *ibid.* **101**, 4778 (1994).
[18] M.M. Kłosek-Dygas, B.J. Matkowsky, and Z. Schuss, Ber. Bunsenges. Phys. **95**, 331 (1991).
[19] P. Talkner, Chem. Phys. **180**, 199 (1994).
[20] D. Ryter, J. Stat. Phys. **49**, 751 (1987).
[21] R.S. Larson and M.D. Kostin, J. Chem. Phys. **69**, 4821 (1978); **77**, 5017 (1982); O. Edholm and O. Leimar, Physica A **98**, 313 (1979); W. Bez and P. Talkner, Phys. Lett. A **82**, 313 (1981).
[22] P. Talkner and E. Pollak, Phys. Rev. E **47**, R21 (1993); E. Pollak and P. Talkner, *ibid.* **47**, 922 (1993).
[23] V.I. Mel'nikov, Phys. Rev. E **48**, 3271 (1993); H. Dekker and A. Maassen van den Brink, *ibid.* **49**, 2559 (1994).
[24] H. Risken, *The Fokker-Planck Equation* (Springer, Berlin, 1989).
[25] G.J. Moro, J. Chem. Phys. **103**, 7514 (1995).
[26] A.N. Drozdov, J. Phys. A **28**, 445 (1995).